Supplementary Information

The band structure and density of states of $CsPbX_3$(X=Cl, Br, and I) are calculated, as shown in Fig. S1(a-c), without considering the SOC effect. Obviously, with the increase of halogen atom radius, the band gap of $CsPbX_3$ gradually decreases, which are 2.12 eV, 1.79 eV, and 1.37 eV respectively, but they all show a direct band gap.

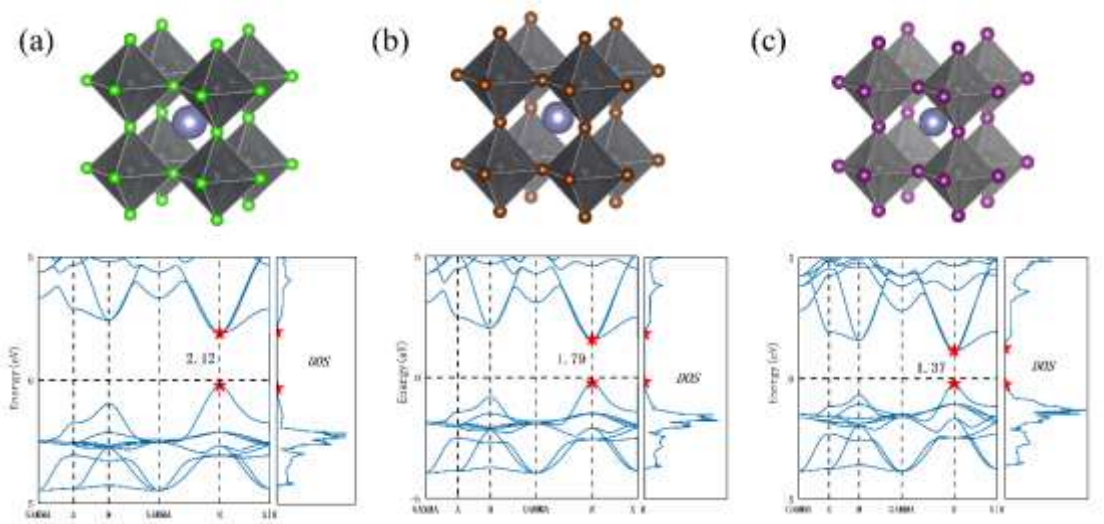

Fig. S1. The band structure and density of states of $CsPbX_3$, without considering the SOC effect. (a)$CsPbCl_3$, (b)$CsPbBr_3$, (c)$CsPbI_3$.

In this work, the adsorption characteristics of several gases on the surface of $CsPbX_3$ are studied, and common low-index surfaces of cubic $CsPbX_3$ are considered, including (100), (110), and (111) surfaces. However, in previous studies, it was shown that the (110) and (111) surfaces are less stable than the (100) surfaces due to the presence of polarity. Therefore, the adsorption performance is studied only on the $CsPbX_3$ (100) surface. Interestingly, along the [100] direction, $CsPbX_3$ shows –[CsX-PbX_2]– layer stacking order (Fig. S2). This stacking order results in two terminations on the (100) surface, labeled as $CsPbX_3$-CsX and $CsPbX_3$-PbX_2, respectively. The electrostatic potentials are calculated to evaluate two different

terminations, as shown in Fig. S3(a–f). The results show that the work functions of the $CsPbX_3$-PbX_2 terminations are 5.17 eV, 5.41 eV, and 5.47 eV, respectively, which were larger than 3.09 eV, 3.06 eV, and 2.46 eV for the $CsPbX_3$-CsX terminations, respectively. It shows that different terminations will seriously affect the distribution and transport of electrons, resulting in a large difference in the adsorption effect on different terminations. To consider all possible outcomes, the adsorption model will be built on both terminals in the [100] direction.

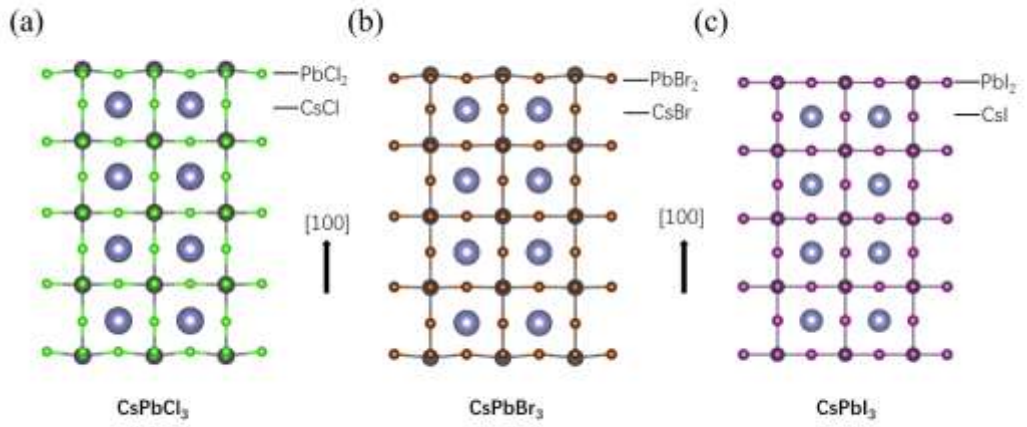

Fig. S2. Two different terminations are stacked along the [100] direction. (a) $CsPbCl_3$, (b) $CsPbBr_3$, (c) $CsPbI_3$.

First of all, the size of all adsorption models is set to 30Å, along the aperiodic direction, and the adsorption distance between the gas and the substrate is set to 3Å. In the preliminary calculation, the adsorption substrate is fixed and the gas molecules are released. When all adsorption models satisfy the convergence criteria, according to the principle that the more negative the adsorption energy is, the more stable the structure is, and the five most stable adsorption models are selected. Tables (S1–S5)

show the adsorption energies of all adsorption models for the five gases, respectively, and the model with the most negative adsorption energy is marked in red.

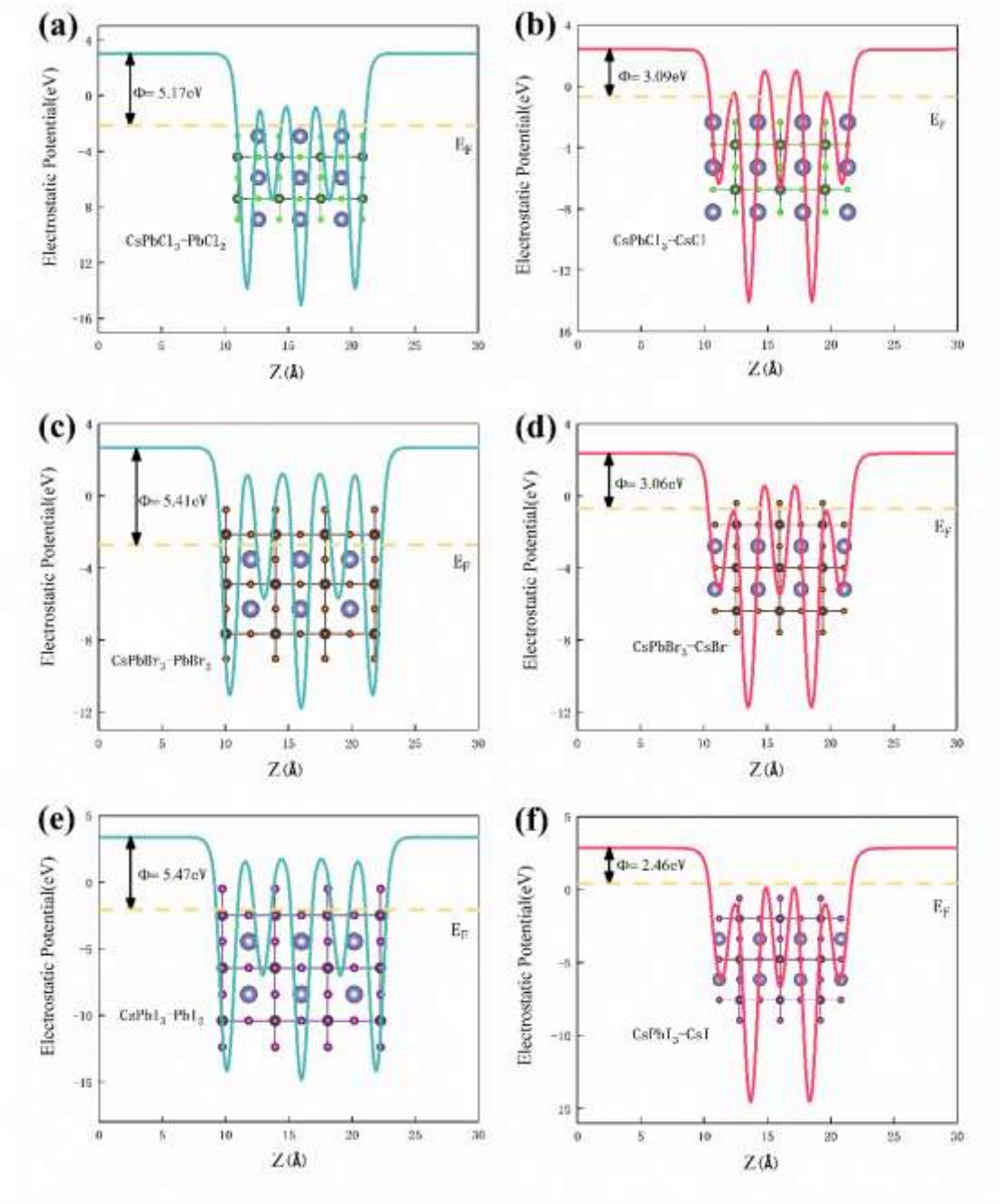

Fig. S3. Planar average of electrostatic potential energies for two terminations of $CsPbX_3$. (a, b) $CsPbCl_3$, (c, d) $CsPbBr_3$, (e, f) $CsPbI_3$.

Then, the maximum adsorption energies of each gas on different terminals are summarized in Table S6. From the point of view of the adsorption substrate, the adsorption energies of all adsorption models on $CsPbI_3$ are around -0.3 eV, which

cannot be used as gas sensing materials. However, when $CsPbBr_3$ is used as the adsorption substrate, the adsorption energy of CH_2O on two different terminals is significantly higher than that of the other four gases. Based on previous research reports, we can preliminarily believe that $CsPbBr_3$ may have potential advantages in the field of CH_2O sensors. For the $CsPbCl_3$ material, the adsorption energy of CH_3OH on its surface is much higher than that of other gases, and the adsorption effect on the $PbCl_2$ terminal is higher than that on the CsCl terminal. However, compared with the adsorption energy of five gases on $CsPbBr_3$, the gas sensing performance of $CsPbCl_3$ is inferior to that of $CsPbBr_3$. In addition, from the point of view of gas, the best model should be the one that meets the maximum adsorption energy of the same gas on different substrates. In short, our final study was performed on these five most stable adsorption models, including C_2H_6/$CsPbBr_3$-$PbBr_2$, CH_4/$CsPbBr_3$-CsBr, CH_3OH/$CsPbCl_3$-$PbCl_2$, CH_3CHO/$CsPbCl_3$-$PbCl_2$, and CH_2O/$CsPbBr_3$-$PbBr_2$. Although the adsorption model of this work is not built on the same adsorption substrate, it still satisfies that the adsorption behavior between the gas and the adsorption substrate is the most stable.

Finally, a fine optimization with the convergence criterion of -0.01 eV/Å is performed on these optimal adsorption models of five gases, and release the three layers on the surface of the adsorption substrate. Finally, when the relaxation processes of the five models reach the convergence state, the relevant adsorption properties are calculated.

Table S1 The total energy(E) of all CH_3OH/$CsPbX_3$ adsorption models, and the red data indicates the energy of the optimal model.

Gas	E(eV)

molecule	-$PbCl_2$	-CsCl	-$PbBr_2$	-CsBr	-PbI_2	-CsI
	-220.773	-204.353	-203.874	-190.411	-184.693	-173.640
CH_3OH	-220.738	-204.583	-203.878	-190.245	-184.660	-174.031
	-220.362	-203.851	-203.885	-190.174	-184.210	-174.072

Table S2 The total energy(E) of all C_2H_6/$CsPbX_3$ adsorption models, and the red data indicates the energy of the optimal model.

Gas molecule	E(eV)					
	-$PbCl_2$	-CsCl	-$PbBr_2$	-CsBr	-PbI_2	-CsI
	-230.872	-214.645	-212.794	-199.864	-195.075	-184.153
C_2H_6	-230.763	-214.214	-214.317	-200.764	-194.113	-184.432
	-230.698	-214.130	-213.495	-200.790	-194.976	-184.319

Table S3 The total energy(E) of all CH_4/$CsPbX_3$ adsorption models, and the red data indicates the energy of the optimal model.

Gas molecule	E(eV)					
	-$PbCl_2$	-CsCl	-$PbBr_2$	-CsBr	-PbI_2	-CsI
	-214.295	-198.053	-197.246	-184.386	-177.569	-167.630
CH_4	-214.472	-198.156	-197.185	-184.530	-177.781	-167.731
	-214.112	-198.243	-197.296	-184.180	-178.463	-167.736

Table S4 The total energy(E) of all CH_3CHO/$CsPbX_3$ adsorption models, and the red data indicate the energy of the optimal model.

Gas molecule	E(eV)					
	-$PbCl_2$	-CsCl	-$PbBr_2$	-CsBr	-PbI_2	-CsI
	-229.212	-212.512	-212.671	-199.376	-193.315	-182.660
CH_3CHO	-229.681	-213.252	-212.871	-199.410	-193.693	-182.900
	-229.276	-213.358	-212.131	-199.322	-192.692	-182.623

Table S5 The total energy(E) of all CH_2O/$CsPbX_3$ adsorption models, and the red data indicates the energy of the optimal model.

Gas	E(eV)

molecule	-$PbCl_2$	-CsCl	-$PbBr_2$	-CsBr	-PbI_2	-CsI
	-212.402	-196.584	-192.144	-182.694	-176.214	-165.995
CH_2O	-212.173	-196.312	-192.542	-182.485	-176.601	-165.741
	-211.897	-196.099	-192.552	-182.586	-176.314	-163.997

Table S6 The maximum adsorption energy of five gases on different substrates.

material	termination	C_2H_6	CH_2O	CH_3OH	CH_4	CH_3CHO
$CsPbBr_3$	-$PbBr_2$	-0.43	-0.54	-0.27	0.14	-0.35
	-CsBr	-0.27	-0.52	-0.16	-0.47	-0.25
$CsPbCl_3$	-$PbCl_2$	-0.33	-0.2	-0.4	-0.39	-0.41
	-CsCl	-0.22	-0.5	-0.43	-0.28	-0.29
$CsPbI_3$	-PbI_2	-0.3	-0.24	-0.26	-0.22	-0.35
	-CsI	-0.3	-0.31	-0.31	-0.17	-0.23

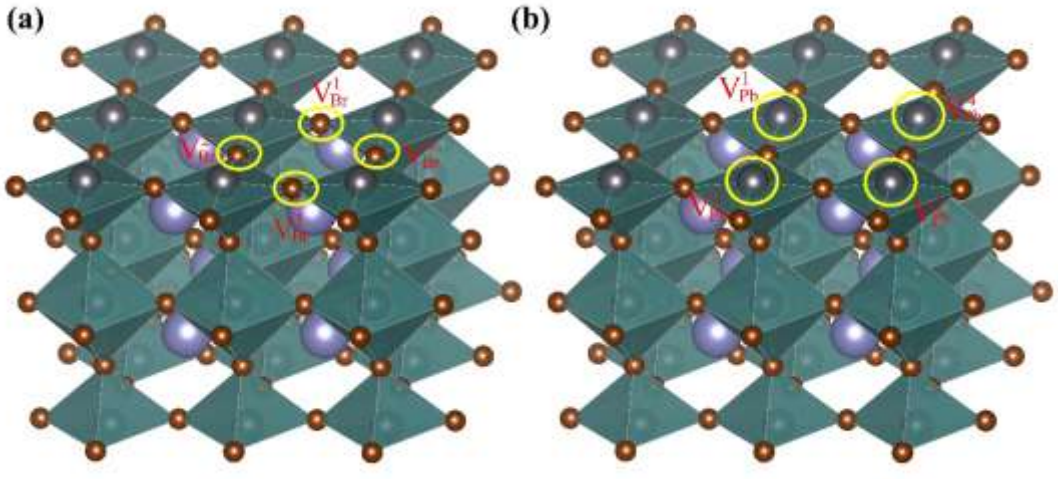

Fig. S4. Different defect sites (a) Br defect, (b) Pb defect.

Table S6 The base energy of the defect model, the energy of the gas/base adsorption system, and the Pb-O distance before and after adsorption.

Defect	E(eV)	P-O distance	Covalent

type	before	after	before	after	radius
V_{Br}^{1}	-159.48	-191.69	3.92	2.81	2.55
V_{Br}^{2}	-159.48	-191.66	3.90	2.82	
V_{Br}^{3}	-159.49	-191.64	3.88	2.78	
V_{Br}^{4}	-159.48	-191.65	3.91	2.86	
V_{Pb}^{1}	-156.42	-188.27	/	/	
V_{Pb}^{2}	-156.43	-188.48	3.92	2.85	
V_{Pb}^{3}	-156.43	-188.29	3.93	3.99	
V_{Pb}^{4}	-156.43	-188.30	3.92	2.81	

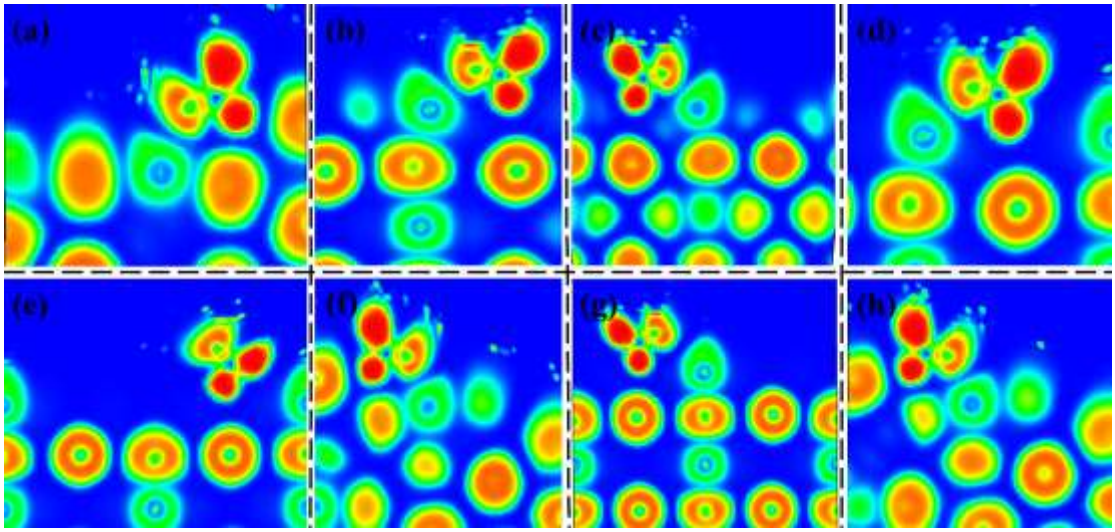

Fig. S5. ELF of adsorption model with defects.